applied sciences

MDPI

Article

Evaluation of the Performance of Pervious Concrete Inspired by CO_2-Curing Technology

Murugan Muthu and Łukasz Sadowski *

Department of Materials Engineering, Wroclaw University of Science and Technology, 50-372 Wrocław, Poland; murugan.muthu@pwr.edu.pl

* Correspondence: lukasz.sadowski@pwr.edu.pl; Tel.: +48-713-203-742

Abstract: Urban runoff is acidic in nature and mainly consists of heavy metals and sediments. In this study, the pervious concrete samples were cured in a CO_2-rich environment and their performance under runoff conditions was evaluated by passing different solutions containing clay particles, heavy metal ions, and acid species. The compressive strength of these samples was reduced by up to 14% when they were cured in water instead of a CO_2 environment. Heavy metal ions, including lead and zinc, in the simulated runoff were adsorbed in these pervious concrete samples by up to 96% and 80% at the end of the experiment, but the acid species in this runoff could leach calcium ions from the cement components during passage. Clay particles in the runoff were trapped in the flow channels of samples, which marginally reduced the percolation rate by up to 14%. Concrete carbonation reduced the release of calcium ions under runoff conditions, and zinc removal was relatively lower because of the nonavailability of hydroxyl sites in the interconnected pore structure. The weight and strength losses in the carbonated concrete samples were relatively lower at the end of the acid storage experiment, suggesting that CO_2 curing reduces cement degradation in aggressive chemicals. The SEM and tomography images revealed the degraded microstructure, while the XRD results provided data on the mineralogical changes. CO_2 curing improves the strength gain and service life of pervious concrete in runoff environments.

Keywords: pervious concrete; carbonation; urban runoff; pore clogging; heavy metal removal

check for updates

Citation: Muthu, M.; Sadowski, Ł. Evaluation of the Performance of Pervious Concrete Inspired by CO_2-Curing Technology. *Appl. Sci.* **2024**, *14*, 4202. https://doi.org/10.3390/app14104202

Academic Editor: Chao-Wei Tang

Received: 30 April 2024
Revised: 13 May 2024
Accepted: 13 May 2024
Published: 15 May 2024

Copyright: © 2024 by the authors. Licensee MDPI, Basel, Switzerland. This article is an open access article distributed under the terms and conditions of the Creative Commons Attribution (CC BY) license (https://creativecommons.org/licenses/by/4.0/).

1. Introduction

Urban runoffs are increasing worldwide due to changing climate and the reduction of pervious areas. The application of pervious concrete pavements mitigates this environmental problem, as it provides opportunities to infiltrate runoff on site as source control measures [1]. This road surface is a good thermal insulator and is pervious but exhibits a lower compressive strength [2]. Prefabrication promotes higher quality control, and pervious concrete components manufactured in a controlled factory environment are gradually attracting attention among road owners because they exhibit relatively higher compressive strength and long-term durability. Cement, water, and stone chips are used to produce pervious concrete mixes [2]. Cement and water are proportioned in smaller amounts to coat and bind crushed aggregates [3]. Cement production and aggregate mining leave a carbon footprint on our planet. The prefabrication industry promotes CO_2-cured pervious concrete components to construct low-traffic road pavements, walkways, and parking lots, as their applications in urban cities can effectively manage runoff and significantly reduce CO_2 emissions [4].

Researchers have proposed the accelerated carbonation method to cure pervious concrete mixes [5], which is a process to accelerate the reaction between CO_2 gas and concrete cementitious materials at a certain gas pressure and CO_2 concentration [6]. This reaction reduces the pH in the pore water of the cement matrix from pH 13 to approximately pH 8 [7]. CO_2 curing of cement-based materials can be understood as a carbon capture

and storage process that involves the reaction of CO_2 with calcium-containing compounds, such as portlandite ($Ca(OH)_2$), calcium silicate hydrate (CSH), tricalcium silicate (C_3S), and dicalcium silicate (C_2S), and the formation of stable carbonates (i.e., $CaCO_3$), as listed in Equations (1)–(4) [8].

$$Ca(OH)_2 + CO_2 = CaCO_3 + H_2O \quad (1)$$

$$CSH + CO_2 = CaCO_3 + SiO_2 + nH_2O \quad (2)$$

$$C_3S + (3 - x)CO_2 + yH_2O = C_xSH_y + (3 - x)CaCO_3 \quad (3)$$

$$C_2S + (2 - x)CO_2 + yH_2O = C_xSH_y + (2 - x)CaCO_3 \quad (4)$$

Carbonation during concrete curing accelerates cement hydration and leads to a higher calcite content and increased strength [9]. There are several merits in the curing of prefabricated pervious concrete in a CO_2-rich environment [10]. The interconnected pore channels within the pervious concrete increase the contact area between CO_2 and the cement matrix, accelerating the diffusion of CO_2 into the cement matrix, and, subsequently, carbonation can occur homogeneously in the material [11]. Furthermore, pervious concrete is applied in a moist environment and flows through water, and leaching damage is a potential risk that cannot be ignored [12]. Concrete curing in a CO_2 environment can fix calcium in insoluble carbonates rather than portlandite, preventing the occurrence of calcium leaching, which is a combined diffusion and dissolution process in which cement hydrates dissociate due to the diffusion of ions driven by the concentration gradient between the alkaline pore solution and external acid solution [13]. Reduced calcium ion concentration in the pore solution leads to the further dissolution of portlandite and CSH to supply calcium ions to maintain equilibrium [14]. The relationship between calcium ion concentrations in solid phases and the pore solution is well known [15]. Carbonation curing densifies the cement microstructure in pervious concrete [11], inhibits the diffusion of ions outward into the pore solution [16], and delays the leaching process [17].

Typically, the runoff from urban city roads is acidic and contains mainly sediments, heavy metals, hydrocarbons, phosphorus, oil, and nitrogen [18]. Runoff containing suspended particles clogs pores within pervious concrete pavements during their lifetime [19]. Heavy metal percolation greatly affects groundwater reserves [20]. The two most fundamental components of pervious concrete are cement paste and aggregate, and both have the individual capacity to adsorb heavy metal ions from aqueous environments [21]. Cement is well known as a soil stabilizer for use in the sequestration of heavy metals in soil mixing [22]. The hydration of cement produces highly alkaline conditions and causes heavy metal ions in urban runoff to immobilize with CSH gel and portlandite crystals, which are the main products formed due to the mixing of cement with water [23]. Despite heavy metal immobilization within concrete, some studies show the risk of heavy metal leaching from cement products containing solid waste, especially when exposed to flowing water [24]. Hardened cement paste is severely attacked by such conditions, causing a decrease in the alkalinity of the cement matrix and the degradation of the main cement hydrates [25], leading to the desorption of immobilized heavy metals from the cement matrix. Carbonation is considered beneficial for the resistance to metal ion leaching of cement-based materials [5]. Carbonation is known to be an important factor that affects the formation of cement hydrates [26], as well as the composition and alkalinity of the cement matrix [27]. Heavy metals, originally presenting as hydroxides in the matrix, are progressively converted to carbonates, thus changing their solubility [28]. To date, laboratory research has been conducted primarily to evaluate the mechanical performance of CO_2-cured pervious concrete mixes [29], but studies on understanding the behavior of such mixes against urban runoff conditions and aggressive chemicals are still lacking to the best of our knowledge.

This study demonstrated the removal of suspended solids and toxic heavy metals from simulated runoff conditions in pervious cement concrete samples cured in a CO_2-rich environment. X-ray tomography and falling head permeameter were used to evaluate the

pore-related properties of these samples, while the characteristics of the simulated runoff solutions were examined with the help of inductively coupled plasma mass spectrometry (ICP-MS), turbidity, and pH meters. A phenolphthalein indicator was sprayed to locate carbonated regions in the pervious concrete samples, and the results of the X-ray diffraction (XRD) and scanning electron microscopy (SEM) studies reveal an alteration in the concrete microstructure due to exposure to CO_2. An acid attack experiment was also performed on such samples to evaluate the effect of concrete carbonation on the degradation properties, including weight and compressive strength losses. These experimental findings allow us to understand the beneficial role of CO_2 treatment in the performance of pervious pavement mixes under runoff conditions and aggressive chemicals.

2. Materials and Methods

2.1. Sample Preparation

Portland cement of CEM I 52.5R grade, according to EN 197-1 [30], was used in the preparation of the pervious concrete samples in this study. The cement sample was tested using the Cilas 1090 model particle size analyzer. Figure 1 shows the size distribution of the cement particles, and the average size was calculated to be 128 µm. The cement samples were passed through a 45 µm sieve, and the passed material was analyzed using Bruker D8 XRD (Billerica, MA, USA) and JEOL JSM-6610A SEM (Tokyo, Japan) to obtain information on morphology and mineralogy. XRD was performed with a Cu Kα source, and the sample was scanned at a rate of 0.02° 2θ per min. The sample was mounted on a steel stub using a carbon adhesive, coated with gold for 60 s, and scanned with the SEM operated at 20 kV to obtain the secondary electron (SE) image. These SEM and XRD results are also illustrated in Figure 1.

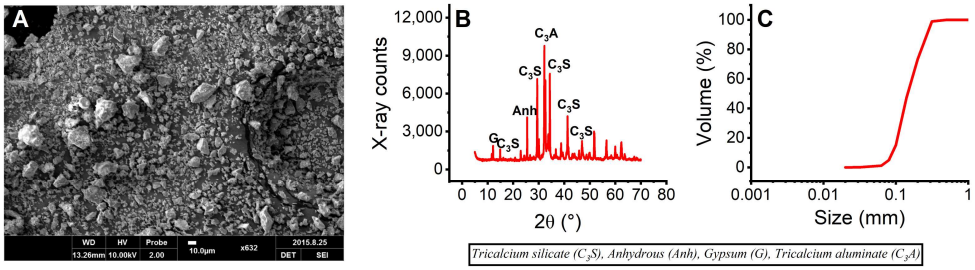


Figure 1. (**A**) SEM image, (**B**) XRD pattern, and (**C**) size distribution of cement particles.

The cement particles were found to have an angular structure and consist mainly of calcium silicates. Granite-derived crushed aggregates, potable water, and a polycarboxylate-ether-based superplasticizer were used in addition to cement to prepare the concrete samples. The water absorption and specific gravity of these aggregates were determined to be 0.42% and 2.77 and were determined according to the European testing standard [31]. The quantities of liquid admixture, water, cement, and aggregate used to prepare 1 m^3 of concrete mixture were 0.3, 34.7, 100, and 450 kg. Aggregates up to 8 mm in size were used to prepare the concrete mixture and were not well graded, as shown in Table 1, to obtain an improved rate of water percolation. The raw materials were mixed in a 60 l tilt-type concrete mixer in a laboratory environment for 4 min. The fresh sample was filled in three equal layers in an iron mold sized 100 mm in diameter and 200 mm in length. A Marshall hammer was used to compact each concrete layer. The diameter, weight of the drop, and free fall of this hammer were 98.4 mm, 4.54 kg, and 457 mm. Twenty-five hammer blows were applied after filling each layer. The upper surface of the fresh sample was smoothed with a tapping knife and then left undisturbed for 24 h.

Table 1. Gradation of crushed aggregates.

Sieve Size in mm	0.3	1.18	2.36	4.75	9.5	12.5	19	25
Passing in %	5	5	25	45	100	100	100	100

Fresh concrete samples were demolded after 24 h of casting and cured in water for up to 28 days. The other set of demolded samples was dried in the laboratory environment for up to 7 days and stored in a 1200 L capacity concrete carbonation chamber of the ThermoScientific model for up to 28 days. The CO_2 concentration, temperature, and relative humidity inside the chamber were maintained at 2%, 25 °C, and 65% during this storage period. This storage experiment was conducted at normal atmospheric pressure. Figure 2 shows the various stages involved in the preparation of these concrete samples.

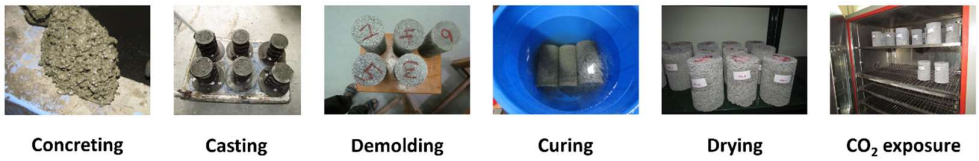


Figure 2. Various stages involved in the preparation of pervious concrete samples.

2.2. Percolation Rate Testing

Figure 3 shows the details of the permeameter setup that was used to measure the percolation rate. The length of the concrete sample was reduced to 150 mm with the use of a diamond-tipped precision saw. The cut sample was enclosed in a latex rubber membrane and mounted on the permeameter using steel clamps and a flexible connector, and tap water was passed in multiple cycles to measure the rate of water percolation. This test procedure has already been elaborated by Muthu and Sadowski [32]. The time taken between the different levels in the initial and final water was measured to calculate the percolation rate according to Darcy's law. Figure 3 shows the permeameter test setup.

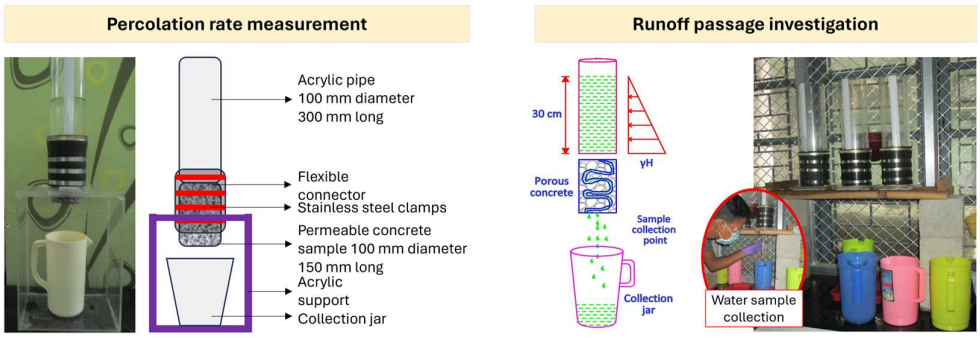


Figure 3. Details of the percolation rate and runoff passage experiments.

2.3. Runoff Passage Testing

Aqueous solutions dissolved with 70% concentrated HNO_3 and lead nitrate and zinc sulfate salts were prepared using analytical grade reagents obtained from Merck. These solutions, each of 2.5 L capacity, were passed through the concrete samples mounted on the permeameter setup for ten repeat cycles. A 10 mL quantity of water sample was collected at the end of every cycle and used for further investigation. The water samples were filtered using a 0.45 µm disk filter, diluted 1000 times, acidified with 2% HNO_3, and analyzed using ICP-MS of the Perkin Elmer NexION-300X model to detect the concentration of calcium, lead, and zinc ions dissolved in them. These metal ions of up to 10^{-5} mg/L can be detected with the ICP-MS used in this study because argon was used as the plasma source and operates at a flow rate of 18 L/min. The pH and turbidity of these water

samples were also measured using battery-operated laboratory devices of the Eutech model. The pH meter was calibrated at three points (pH 4.01, 7, and 9.21), while the turbidity meter was calibrated at four points (turbidity 0.02, 20, 100, and 800 NTU), according to the NIST and ISO guidelines. Sodium-based bentonite clay powder was obtained from a local chemical supplier and thoroughly mixed in distilled water to obtain highly turbid water, which was later passed through concrete samples for ten repeat cycles to obtain information on the reduction in concrete permeability. The average size of this clay reported by the manufacturer was 10 μm. Figure 3 also shows the details of this runoff passage investigation.

2.4. Acid Attack

A 40 mm diameter and 100 mm long pervious concrete sample was extracted from the cast samples using a diamond-tipped core drill machine. Cut samples were stored in a 1000 mL capacity glass beaker containing a HNO_3 solution of 0.5 molar concentration for up to four weeks. This storage experiment was conducted to assess the performance of carbonated concrete stored in aggressive chemicals. The HNO_3 solution was replenished at the end of each week. This relatively high concentration of acid was used to facilitate the generation of data in a short time by accelerating sample degradation. The loss in sample weight at the end of the acid attack was recorded using a 0.001 g precision weighing balance.

2.5. Characterization Studies

To obtain information on pore-related properties, the cut sample of 40 mm in diameter was scanned with a 3D X-ray computed tomography (CT) operated with a cesium iodide flat panel detector at 120 kV and 70 μA. A GE-phoenix model CT was used in this study, and the X-ray scan was collected at a rate of 4 ms per image. Phoenix CT acquisition software was used to obtain the resulting 2D radiographs, which were then reconstructed using VGStudio-Max software. The final 3D tomograph was sectioned into 100 slices using image reconstruction software. The fraction of pore area in these 2D sliced images was determined using image analysis software, and this analysis procedure has been elaborated by Muthu and Sadowski [32]. The image analysis directly gives the pore size and its distribution. The pore area fraction (i.e., surface porosity of the sample) in each sliced image was calculated with these data, and the average was calculated. Figure 4 shows the various stages of this image analysis method. To examine the effect of CO_2 and acid on the microstructure of the cement matrix, XRD and SEM studies were carried out on concrete samples destroyed in the compression test machine. Tiny pieces were collected and ground to a size smaller than 45 μm using a mortar and pestle and a standard sieve. Care was taken to avoid aggregate particles during this sample collection and preparation. An X-ray scan was taken on the powdered sample for a 5–80° 2θ range. The obtained cement fragments were mounted on the steel stub, gold-coated, and scanned with the SEM operated at 20 kV to obtain SE images.

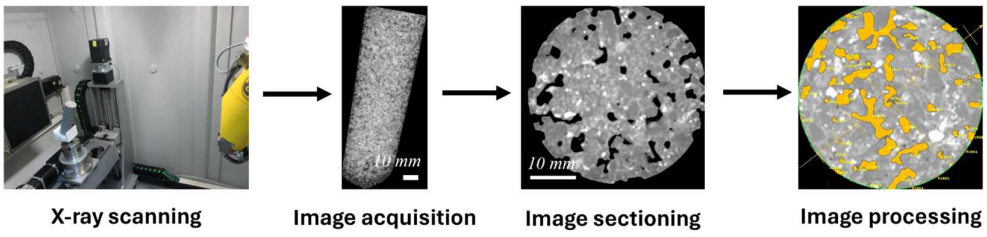


Figure 4. Flow of steps in tomography image acquisition and processing.

3. Results and Discussion

3.1. Concrete Carbonation

The pH of the potable water used to cure the concrete samples increased from 8.01 to 12.21 due to the dissolution of free lime and $Ca(OH)_2$ from the porous matrices. When

these samples were cured in the CO_2 chamber instead of in water, this pH increase was relatively lesser. The average compressive strength of concrete samples cured in water and the CO_2 environment was found to reach 27.34 and 31.23 MPa at the end of 28 days. A compressive strength test was carried out on a sulfur-capped concrete sample of 100 mm in diameter and 150 mm in length according to the procedure already explained by Muthu and Sadowski [32]. In this study, there is an increase in concrete strength of up to 14% due to the continuous storage of porous samples in a CO_2 environment. There is no significant difference in the rate of percolation of water through these samples as a result of variations in the curing conditions. The average percolation rate was calculated to be 18 L/min/m^2. The standard deviation of these measurements was found to be 3.2 L/min/m^2. CT images of these samples were analyzed to determine their surface porosities. It is well known that the performance of any pervious medium is inherently dependent on the properties of its pore structure [33]. The total volume and size distribution of the pores and the interconnectivity of the pores phase in pervious concrete determine its performance characteristics [34].

The CT slice shown in Figure 5 reveals the random distribution of pores along the length of the concrete sample in this study. The greyscale value of the CT image differentiates the concrete components. The black regions in this section refer to the voids, the white regions refer to the very dense anhydrous compounds, and the grey regions indicate the formed cement hydrates. The distribution of the pore area fraction (i.e., surface porosity) along the sample length was found to fall within the range of 6–28%. The average pore area fraction of non-carbonated and carbonated samples was calculated to be 16.4% and 14.8%. The difference in these porosities was found to be very low, which explains why the curing condition did not influence the interconnected pore structure. The rate of the percolation of water is the most important characteristic of the performance of pervious concrete [35]. Concrete transport properties are inherently dependent on the characteristics of the pore structure [36]. However, it has been common to relate the permeability of pervious concrete with its porosity, primarily due to the ease with which porosity can be measured in such a porous material [37].

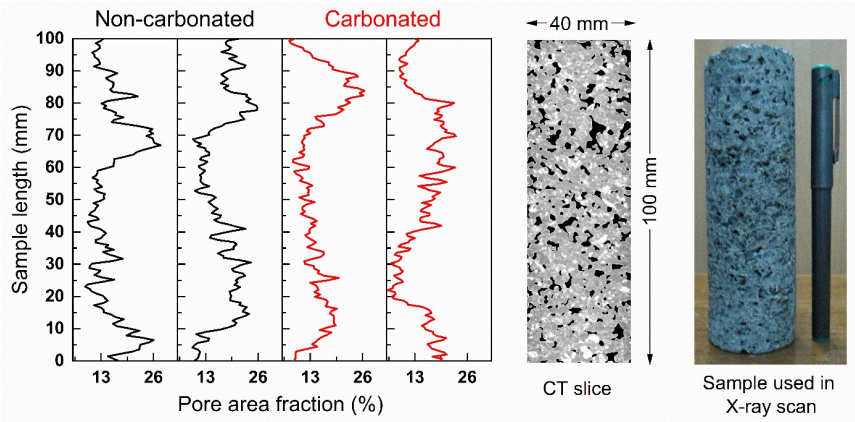


Figure 5. Porosity distribution along the length of pervious concrete samples.

In this study, the concrete sample was divided into two halves using a cutting tool, and a solution of phenolphthalein indicator obtained from Merck was sprayed onto the inner cut surfaces to locate the carbonated regions. Figure 6 shows the fractured surface of the freshly cut pervious concrete samples at the end of CO_2 exposure. Spraying the phenolphthalein solution on the cut section of carbonated samples resulted in a colorless effect, indicating a pH less than 8.2. The CO_2 gas easily penetrates the macropore channels and seems to carbonate all the cement surfaces prevailing in the interconnected pore structure. The phenolphthalein changed from colorless to pink on water-cured concrete surfaces when the pH was above 9.5. The carbonization process is a chemical reaction that takes place in concrete, involving calcium-containing compounds and CO_2, leading to the formation of stable $CaCO_3$ and water [38]. This reaction results in the depletion of

hydroxides, primarily $Ca(OH)_2$, which reduces the pH of the concrete pore solution [39]. Calcite is 17% larger in size than portlandite, inducing structural changes in the cement matrix [9]. It is worth mentioning that cement-based materials cured in a CO_2 environment are different from concrete carbonation, and their main reactions and influencing factors are naturally different [40]. Carbonation curing is related to the development of strength, microstructure densification, and mitigation of chemical attack, but the decrease in alkalinity raises concerns about the corrosion issue of steel bars [40]. Pure CSH, portlandite, and ettringite in powder form rapidly carbonate at high relative humidity, while the pore structure, relative humidity, drying state, and degree of water saturation inside the concrete pore system play a significant role in the carbonation of solid concrete components [41]. The bonding of the CSH surfaces to the calcium ions in the calcite is very strong, thus improving the compressive strength [42]. Calcite crystals of significant volume are usually seen in the microstructure of CO_2-cured concrete but not in water-cured concrete. Three types of $CaCO_3$, including calcite, vaterite, and aragonite, form in concrete exposed to CO_2 at an early stage. The prolongation of this CO_2 exposure transforms vaterite and aragonite into more stable calcite [42].

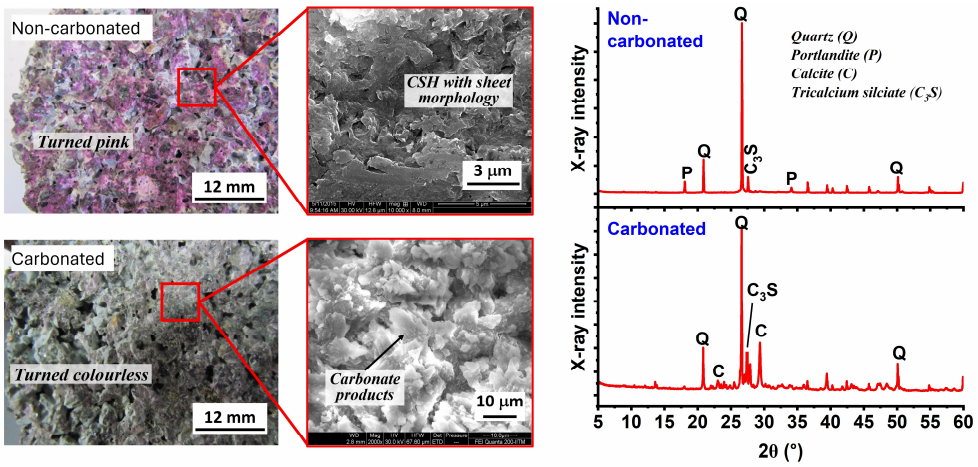


Figure 6. SEM and XRD results, which reveal the mineralogy of carbonated concrete.

The SEM and XRD results shown in Figure 6 provide morphological and mineralogical information on the pervious concrete surfaces cured with water and CO_2. CSH with sheet morphology was observed in the microstructure of the water-cured sample, while rhombohedral $CaCO_3$ crystals (i.e., calcite) were found in the CO_2-exposed sample. The major X-ray peaks at 18.1°, 26.6°, 27.7°, and 29.4° 2θ positions are attributed to portlandite ($Ca(OH)_2$), quartz (SiO_2), calcium silicates (i.e., unhydrated cement), and calcite ($CaCO_3$), and their presence was observed in the XRD pattern of concrete samples. It is worth mentioning that the powder diffraction file numbers of quartz, calcite, and portlandite crystals, according to the International Center for Diffraction Data, are 46-1045, 5-586, and 5-733. The X-ray peak attributed to portlandite was not found in the carbonated sample XRD result, indicating the conversion of portlandite to calcite during the hardening stage of the sample cured in a CO_2 environment. These findings highlight that CO_2 exposure did not alter the hydraulic conductivity of pervious concrete but helped to form stable carbonates that improved compressive strength. Carbonation involves the change of CO_2 from the gaseous to the aqueous form. The reaction of CO_2 with water led to carbonic acid, which dissociated into protons and carbonates, depending on the pH of the solution [43]. After the dissolution of gaseous CO_2, the precipitation of carbonates with metal cations remained in the solution, provided that the solubility of the metal carbonates was exceeded. The carbonation reaction is very slow in water-saturated concrete because CO_2 diffusion is affected by free water that is filled in the pores. This reaction is also slower in completely

dry pores because the formation of metal carbonates occurs in an aqueous form, often in the film of free water occupying the pores [44].

3.2. Runoff Characteristics

Clay containing water with a turbidity of around 800 NTU was passed through the concrete samples for ten repeat cycles. Figure 7 shows the change in this water turbidity at the end of each cycle and the consequent reduction in the percolation rate due to sediment blockage. The clayey water turbidity at the end of the first cycle was reduced from 800 to 645 NTU. However, the reduction in this water turbidity in subsequent cycles was not significant regardless of the different curing conditions used in the preparation of the sample. The percolation rate was found to gradually reduce with increasing test cycles. The reduction in percolation rate at the end of the experiment reached 86% and 91% in the case of non-carbonated and carbonated samples. As illustrated in Figure 7, clay particles may have occupied the dead-end pores of the concrete matrices during passage, which was the reason for the minor reduction in turbidity and the rate of water percolation. Clayey particles are associated with each other by the van der Waals attractions between them, and the increase in their densities severely reduces water percolation in pervious concrete [45]. Clay-induced pore clogging is ten times greater than that caused by sand [46]. The size of the pores in the pervious concrete is in the range of 2–8 mm [2]. Pervious concrete reduces surface runoff and maximum flow by 30% and 70%, but during service, the pores in this concrete gradually become clogged with silt, sand, and organic matter, affecting hydraulic performance [47]. These clogged particles also accumulate fine pores in the matrix, and when dried, they form a hard crust that seals the pores. The level of water percolation through pervious concrete is reduced due to these processes, causing surface overflow and ponding when infiltration rates are less than the intensity of rainfall [48]. Cleaning methods that are effective in removing clogged particles from pervious concrete are vacuum cleaning, air compression, and hydro washing. The accumulated sediments at the shallow depths of the pervious concrete pavement are removed with a vacuum cleaner, followed by air compression to expel the grains from the middle section, and finally, hydro washing to remove the adhering sediment and unclog the interconnected pore channels. This combination has been shown to recover water percolation by up to 90% [45].

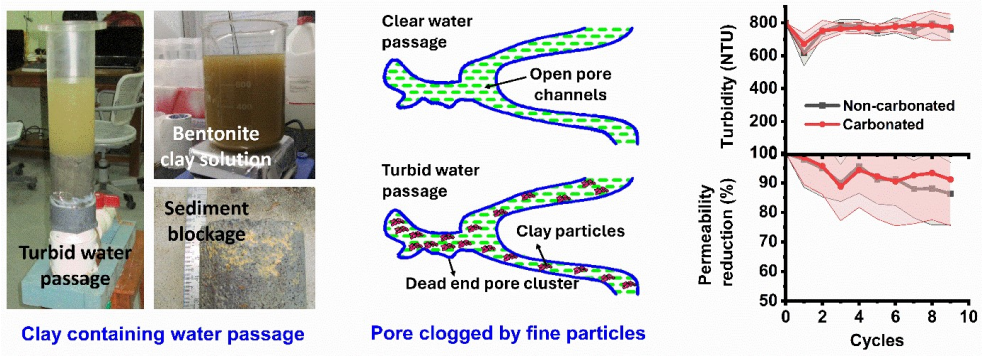


Figure 7. Change in turbidity and percolation rate due to the passage of clay containing water.

Figure 8 illustrates the amount of calcium ions released from pervious concrete samples due to the passage of distilled water and HNO_3 solution for ten repeat cycles. This figure also presents the change in their pH at the end of each cycle. The initial pH of the distilled water and HNO_3 solution was measured to be around 3.21 and 6.94. This examination was carried out mainly to reveal the leaching behavior of carbonated concrete when exposed to acidic species in the simulated runoff. Calcium ions were found to be released from the porous concrete matrices regardless of the curing conditions and characteristics of the percolating water. However, this removal of calcium ions from concrete samples was found to be relatively less when the pervious samples were cured in a CO_2-rich environment. The pH results correlate well with the calcium removal information. The

dissolved sources of calcium ions were mainly derived from $Ca(OH)_2$ and CSH. The pH of the HNO_3 solution and the distilled water that passed through the non-carbonated samples was found to be 11.44 and 11.63 at the end of the experiment. In the case of carbonated samples, the pH values of these solutions were 9.91 and 10.16, respectively. The pH values were found to gradually increase with cycles. The cement surfaces in the flow channels of the pervious concrete are subjected to coupled calcium leaching and hydraulic abrasion due to infiltrating runoff [49]. Calcium leaching gradually degrades the microstructure of these cement surfaces, whereas hydraulic abrasion provides a shearing action and erodes the toxic heavy metal ions of the runoff that have become immobilized on such surfaces. These ill effects reduce the service life of concrete, and detached heavy metal ions pollute the surrounding environment [49].

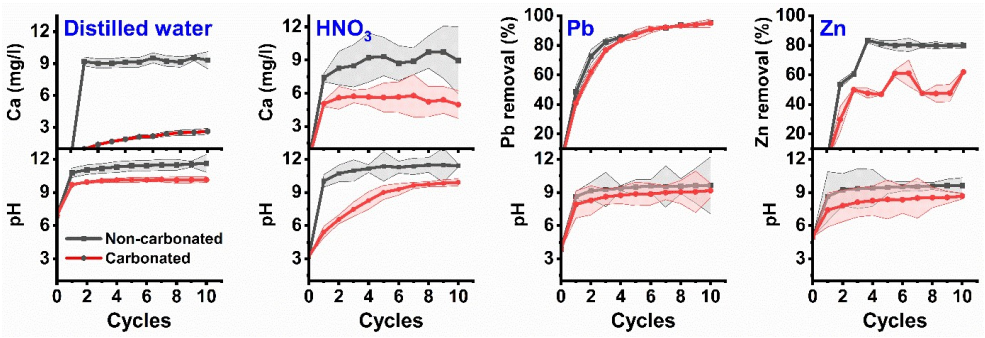


Figure 8. Change in characteristics due to the passage of aqueous solutions simulating urban runoff.

The leaching process is usually controlled by diffusion from within the concrete and ongoing surface dissolution mechanisms [50]. Alkalis in cement matrices are released by diffusion, but calcium release is mainly due to the dissolution of surface portlandite and, at a pH less than 12.4, decalcification of the CSH gel. Calcium release is lower in carbonated concrete because it is transferred from portlandite and CSH to less soluble calcite. A low concentration of alumina and silicates exists in the pores of ettringite and monosulfate, which is why their release is due to the dissolution of these compounds on concrete surfaces. The release of alumina from carbonated concrete is very low because the solubility control is transferred to aluminum hydroxide (i.e., gibbsite). In contrast, ettringite in carbonated concrete dissolves so that additional silicates are released by diffusion out of the carbonated layer [50]. Although percolated water has a pH that exceeds the maximum permissible limits of drinking water according to the WHO standards [51], several soils below the concrete pavement have a modest self-buffering capacity for the attenuation of high-pH water [52].

In this study, aqueous solutions containing lead and zinc were passed through the concrete samples for ten repeat cycles. The concentration of these metal ions in the solutions was limited to 10 mg/L in this study. Figure 8 shows the percentage of removal of these metal ions from concrete samples in each cycle and the subsequent change in the pH of the percolated solutions. The removal of lead and zinc in non-carbonated samples reached 96% and 80% at the end of the experiment. The removal of lead in carbonated samples was found to be almost the same, but the removal of zinc at the end of the experiment was 62%. Zinc removal is reduced when concrete samples are carbonated. This finding indicates that lead adsorption on the hydroxyl and carbonate sites is stronger, but zinc adsorption is relatively stronger on the hydroxyl sites. Zinc precipitation occurs at a pH greater than 8.4 and may have precipitated as $Zn(OH)_2$ as a result of the high neutralizing capacity of the non-carbonated samples. Lead species adsorb strongly onto the surfaces of CSH and calcium silicates and precipitate as lead silicates [53]. Lead carbonate sulfate hydroxide ($Pb_4SO_4(CO_3)_2(OH)_2$) and lead carbonate hydroxide hydrate ($3PbCO_3{\cdot}2Pb(OH)_2{\cdot}H_2O$) form by chemical adsorption of the redissolved lead species in the pore channels of the

pervious concrete [54]. The precipitation of heavy metal hydroxides might be the dominant removal mechanism of pervious concrete samples.

Holmes et al. [55] reported that the removal of lead, zinc, and cadmium in pervious concrete is primarily caused by the localized pH in the pore water due to the hydration of cement compounds. Calcium, hydroxides, sulfates, carbonates, and silicates are readily available in pore water during and after cement hydration in pervious concrete. These ions in the pore solution increase ionic strength and promote reactions that form calcium heavy-metal double hydroxides and heavy-metal carbonates. Secondary removal occurs via sorption, wherein heavy metal hydroxides, produced as a result of the high pH, favorably adsorb onto and then mainly diffuse into the cement matrix. In the case of cement-bound waste, CO_2 curing led to the formation of an improved calcite content and a significant reduction in the leaching of calcium, arsenic, nickel, zinc, copper, lead, chromium, and molybdenum [56]. The leaching of these ions is dependent on the pH and formation of metal carbonates.

3.3. Concrete Degradation

Figure 9 shows the weight and strength losses in the concrete samples at the end of acid storage. The average weight loss (and strength loss) in these samples was calculated to be 28% and 25% (and 53% and 47%) at the end of acid storage, respectively. These findings show the beneficial effect of carbonation on the resistance to calcium leaching of the pervious concrete matrix in aggressive chemicals. An acid attack on traditional concrete usually results in the dissolution of cement components, but the degradation of the aggregate depends on its mineralogy [57]. Hydroxyl ions contained in cement hydrates are neutralized by acid species (i.e., protons). Aluminum, iron, sulfur, and mainly calcium ions enter the pore solution and diffuse to the concrete surface. A highly porous degraded layer is formed consisting of hydrated silicates, and the rate of development of this layer is determined by the diffusion of acid species through the degraded layer to the reaction front and the acid reaction rate with the unaltered core concrete [58]. In this study, the CT image in Figure 9 reveals a significant removal of the cement binder from the porous concrete matrix due to the acid attack. A degraded layer surrounding the unaltered core concrete was not observed, but the presence of granite-derived crushed aggregates and their distribution were clearly seen as a result of the acid attack. A similar observation was observed in non-carbonated and carbonated samples. Although the ingredients are the same in the pervious concrete and traditional concrete, the physical characterization of degradation due to the acid attack was still different due to the formation of an interconnected pore structure.

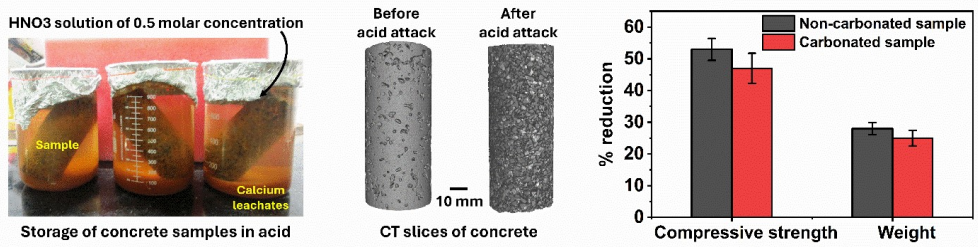


Figure 9. Weight and strength losses in pervious concrete samples due to acid attack.

Figure 10 illustrates the SEM and XRD results that reveal the acid-degraded microstructure of the concrete samples. The CSH structure was completely decalcified, and only silica gel was left as a result of the exposure of the non-carbonated and carbonated samples to acid. The XRD result confirms the presence of porous silica gel in both the non-carbonated and carbonated samples. Chen, Li, Gao, Guo, and Qin [5] found a reduction in the compressive strength of cement paste samples caused by calcium leaching when the samples were carbonated for up to 16 h. These results were found to be contrasting when the carbonation period was prolonged. Limiting early carbonation exposure in cement paste samples can improve calcium leaching resistance by densifying the microstructure and producing stable

$CaCO_3$/silica gel. Severe CSH decalcification occurs in acid-exposed samples carbonated for a longer duration [5]. Two main factors that influence the long-term durability of pervious concrete mixes are porosity and compressive strength. Wu et al. [59] found a strong correlation between porosity and the parameters that control long-term durability, and their findings report that lower porosity pervious concrete provided better resistance to extreme environments. Xiang et al. [60] found a reduction in the bond strength between aggregate particles due to cement degradation in pervious concrete samples exposed to aggressive aqueous species.

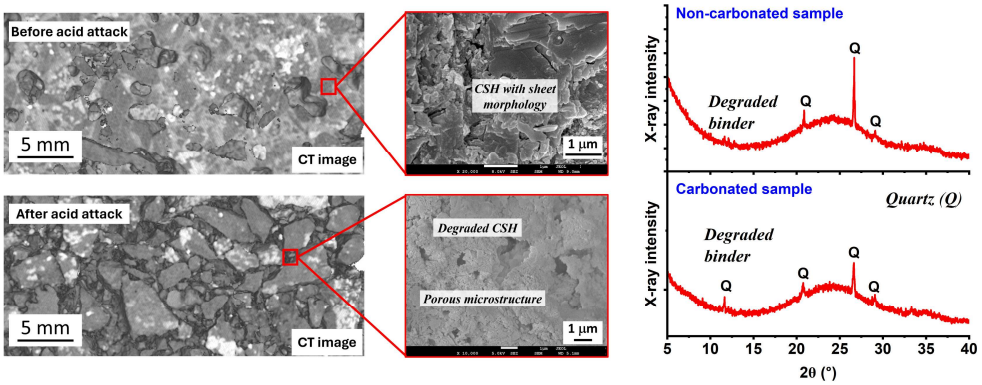


Figure 10. CT, SEM, and XRD results of pervious concrete samples at the end of acid attack.

4. Conclusions

The key experimental findings are listed below:

- The pervious concrete mix developed in this study was able to infiltrate water up to 18 L/min/m^2 and obtained a compressive strength of about 27 MPa at the end of 28 days. This strength increased by up to 14% when the mix samples were cured in a CO_2-rich environment for up to 28 days. This curing environment did not change the infiltration rate and the formation of pores in the pervious concrete;
- CO_2 gas easily penetrated the pervious concrete and was able to carbonate the cement components prevailing on the surface of the interconnected pore structure. This observation was evident in the cut-sample surfaces sprayed with the phenolphthalein indicator. A rich formation of calcite was observed in the microstructure of the carbonated samples;
- The passage of clay-containing bentonite water through them affected the rate of water infiltration because the pores were blocked by clay particles. This finding was observed to be the same in both the non-carbonated and carbonated samples. However, lead removal was excellent in these samples regardless of the curing conditions. Zinc removal in the carbonated and non-carbonated concrete samples reached 62% and 80% at the end of the experiment, indicating that zinc removal was outstanding when the cement matrix contained more hydroxyl sites than carbonate sites;
- Calcium release from the water passage was found to be reduced when portlandite crystals were transformed into stable carbonates due to continuous exposure to CO_2. Calcite solubility under running water conditions was found to be relatively lower than that of portlandite. The acid attack on the pervious concrete samples resulted in the degradation of the cement components, and only aggregates were observed to remain in the porous matrices at the end of the experiment. Their weight and strength losses reached 28% and 53%, but these losses were found to be relatively lower in the case of carbonated samples, highlighting the beneficial effect of CO_2 curing on the resistance to calcium leaching of pervious concrete in aggressive chemicals and urban runoff conditions. The effect of CO_2 curing on concrete degradation in chloride and sulfate exposure attacks will be our future study;

- Prefabricated CO_2-cured pervious concrete components have improved strength and durability, and the application of these environmentally friendly materials as road surfaces can effectively manage runoff and remediate environmental pollution.

Author Contributions: Conceptualization, methodology, validation, formal analysis, investigation, data curation, and writing—original draft preparation, M.M.; resources, supervision, writing—review and editing, Ł.S. All authors have read and agreed to the published version of the manuscript.

Funding: This research was funded by Narodowa Agencja Wymiany Akademickiej (NAWA), grant number BPN/ULM/2021/1/00120.

Institutional Review Board Statement: Not applicable.

Informed Consent Statement: Not applicable.

Data Availability Statement: Data were not used for the research described in the article.

Conflicts of Interest: The authors declare no conflict of interest.

References

1. Goonetilleke, A.; Thomas, E.; Ginn, S.; Gilbert, D. Understanding the role of land use in urban stormwater quality management. *J. Environ. Manag.* **2005**, *74*, 31–42. [CrossRef] [PubMed]
2. ACI 522R. *Report on Pervious Concrete*; American Concrete Institute: Farmington Hills, MI, USA, 2010; p. 42. ISBN 9780870313646.
3. Yang, J.; Jiang, G. Experimental study on properties of pervious concrete pavement materials. *Cem. Concr. Res.* **2003**, *33*, 381–386. [CrossRef]
4. Dauji, S. Thickness Design of Slab-on-Grade Construction: Review of Some Key Aspects. *Pract. Period. Struct. Des. Constr.* **2021**, *26*, 04021029. [CrossRef]
5. Chen, T.; Li, L.; Gao, X.; Guo, M.; Qin, L. New insights into the role of early accelerated carbonation on the calcium leaching behavior of cement paste. *Cem. Concr. Compos.* **2023**, *140*, 105103. [CrossRef]
6. Kim, G.M.; Jang, J.G.; Naeem, F.; Lee, H.K. Heavy metal leaching, CO_2 uptake and mechanical characteristics of carbonated porous concrete with alkali-activated slag and bottom ash. *Int. J. Concr. Struct. Mater.* **2015**, *9*, 283–294. [CrossRef]
7. Garrabrants, A.C.; Sanchez, F.; Kosson, D.S. Changes in constituent equilibrium leaching and pore water characteristics of a Portland cement mortar as a result of carbonation. *Waste Manag.* **2004**, *24*, 19–36. [CrossRef] [PubMed]
8. Sikora, P.; Woliński, P.; Chougan, M.; Madraszewski, S.; Węgrzyński, W.; Papis, B.K.; Federowicz, K.; Ghaffar, S.H.; Stephan, D. A systematic experimental study on biochar-cementitious composites: Towards carbon sequestration. *Ind. Crops Prod.* **2022**, *184*, 115103. [CrossRef]
9. Van Gerven, T.; Van Baelen, D.; Dutré, V.; Vandecasteele, C. Influence of carbonation and carbonation methods on leaching of metals from mortars. *Cem. Concr. Res.* **2004**, *34*, 149–156. [CrossRef]
10. Muthu, M. *Performance of Concrete Based Water Filtration System: Influence of Reduced Graphen Oxide and Accelerated Carbonation*; Indian Institute of Technology Madras: Chennai, India, 2017.
11. Murugan, M.; Santhanam, M.; Kumar, M. Pb removal in pervious concrete system: Effects of carbonation and hydraulic retention time. *Constr. Build. Mater.* **2017**, *174*, 224–232.
12. Muthu, M.; Chandrasekharapuram Ramakrishnan, K.; Santhanam, M.; Rangarajan, M.; Kumar, M. Heavy metal removal and leaching from pervious concrete filter: Influence of operating water head and reduced graphene oxide addition. *ASCE J. Environ. Eng.* **2019**, *145*, 04019049. [CrossRef]
13. Jain, J.; Neithalath, N. Analysis of calcium leaching behavior of plain and modified cement pastes in pure water. *Cem. Concr. Compos.* **2009**, *31*, 176–185. [CrossRef]
14. Manohar, S.; Bala, K.; Santhanam, M.; Menon, A. Characteristics and deterioration mechanisms in coral stones used in a historical monument in a saline environment. *Constr. Build. Mater.* **2020**, *241*, 118102. [CrossRef]
15. Gaitero, J.J.; Campillo, I.; Guerrero, A. Reduction of the calcium leaching rate of cement paste by addition of silica nanoparticles. *Cem. Concr. Res.* **2008**, *38*, 1112–1118. [CrossRef]
16. Mi, R.; Wang, Y.; Yu, T.; Li, W. Effects of carbon-sequestering coral aggregate on pore structures and compressive strength of concrete. *Low-Carbon Mater. Green Constr.* **2023**, *1*, 21. [CrossRef]
17. Tanaka, I.; Koishi, M.; Shinohara, K. A study on the process for formation of spherical cement through an examination of the changes of powder properties and electrical charges of the cement and its constituent materials during surface modification. *Cem. Concr. Res.* **2002**, *32*, 57–64. [CrossRef]
18. Chandrappa, A.K.; Biligiri, K.P. Pervious concrete as a sustainable pavement material—Research findings and future prospects: A state-of-the-art review. *Constr. Build. Mater.* **2016**, *111*, 262–274. [CrossRef]
19. Kayhanian, M.; Anderson, D.; Harvey, J.T.; Jones, D.; Muhunthan, B. Permeability measurement and scan imaging to assess clogging of pervious concrete pavements in parking lots. *J. Environ. Manag.* **2012**, *95*, 114–123. [CrossRef]

20. Kim, G.M.; Jang, J.G.; Khalid, H.R.; Lee, H.K. Water purification characteristics of pervious concrete fabricated with CSA cement. *Constr. Build. Mater.* **2017**, *136*, 1–8. [CrossRef]
21. Giergiczny, Z.; Król, A. Immobilization of heavy metals (Pb, Cu, Cr, Zn, Cd, Mn) in the mineral additions containing concrete composites. *J. Hazard. Mater.* **2008**, *160*, 247–255. [CrossRef]
22. Ma, X.; He, T.; Da, Y.; Lin, Y.; Feng, Y.; Zhang, W. Evaluation of the ability of cement prepared with incineration fly ash to solidify heavy metals at high temperatures. *J. Build. Eng.* **2023**, *78*, 107559. [CrossRef]
23. Haselbach, L.; Poor, C.; Tilson, J. Dissolved zinc and copper retention from stormwater runoff in ordinary portland cement pervious concrete. *Constr. Build. Mater.* **2014**, *53*, 652–657. [CrossRef]
24. Yu, Q.; Nagataki, S.; Lin, J.; Saeki, T.; Hisada, M. The leachability of heavy metals in hardened fly ash cement and cement-solidified fly ash. *Cem. Concr. Res.* **2005**, *35*, 1056–1063. [CrossRef]
25. Wan, K.; Li, Y.; Sun, W. Experimental and modelling research of the accelerated calcium leaching of cement paste in ammonium nitrate solution. *Constr. Build. Mater.* **2013**, *40*, 832–846. [CrossRef]
26. Greco, E.; Ciliberto, E.; Verdura, P.D.; Lo Giudice, E.; Navarra, G. Nanoparticle-based concretes for the restoration of historical and contemporary buildings: A new way for CO_2 reduction in architecture. *Appl. Phys. A* **2016**, *122*, 524. [CrossRef]
27. Park, J.; Kim, Y. Improvement in mechanical properties by supercritical carbonation of non-cement mortar using fly ash and blast furnace slag. *Int. J. Precis. Eng. Manuf.* **2014**, *15*, 1229–1234. [CrossRef]
28. Van Gerven, T.; Cornelis, G.; Vandoren, E.; Vandecasteele, C.; Garrabrants, A.C.; Sanchez, F.; Kosson, D.S. Effects of progressive carbonation on heavy metal leaching from cement-bound waste. *AIChE J.* **2006**, *52*, 826–837. [CrossRef]
29. Chen, T.; Gao, X. Use of carbonation curing to improve mechanical strength and durability of pervious concrete. *ACS Sustain. Chem. Eng.* **2020**, *8*, 3872–3884. [CrossRef]
30. *EN 197-1*; Cement: Composition, Specifications and Conformity Criteria for Common Cements. British Standards Institute: London, UK, 2011; p. 46.
31. *EN 1097-6*; Tests for Mechanical and Physical Properties of Aggregates—Part 6: Determination of Particle Density and Water Absorption. British Standard Institution: London, UK, 2013; p. 49.
32. Muthu, M.; Sadowski, Ł. Performance of permeable concrete mixes based on cement and geopolymer in aggressive aqueous environments. *J. Build. Eng.* **2023**, *76*, 107143. [CrossRef]
33. Sumanasooriya, M.S.; Neithalath, N. Stereology-and morphology-based pore structure descriptors of enhanced porosity (pervious) concretes. *ACI Mater. J.* **2009**, *106*, 429–438.
34. Neithalath, N.; Marolf, A.; Weiss, J.; Olek, J. Modeling the Influence of Pore Structure on the Acoustic Absorption of Enhanced Porosity Concrete. *J. Adv. Concr. Technol.* **2005**, *3*, 29–40. [CrossRef]
35. Neithalath, N.; Sumanasooriya, M.S.; Deo, O. Characterizing pore volume, sizes, and connectivity in pervious concretes for permeability prediction. *Mater. Charact.* **2010**, *61*, 802–813. [CrossRef]
36. Katz, A.J.; Thompson, A.H. Quantitative prediction of permeability in porous rock. *Phys. Rev. B* **1986**, *34*, 8179–8181. [CrossRef] [PubMed]
37. Neithalath, N.; Weiss, J.; Olek, J. Characterizing enhanced porosity concrete using electrical impedance to predict acoustic and hydraulic performance. *Cem. Concr. Res.* **2006**, *36*, 2074–2085. [CrossRef]
38. Huo, Z.; Wang, L.; Huang, Y. Predicting carbonation depth of concrete using a hybrid ensemble model. *J. Build. Eng.* **2023**, *76*, 107320. [CrossRef]
39. Li, L.; Wu, M. An overview of utilizing CO_2 for accelerated carbonation treatment in the concrete industry. *J. CO2 Util.* **2022**, *60*, 102000. [CrossRef]
40. Zhang, D.; Ghouleh, Z.; Shao, Y. Review on carbonation curing of cement-based materials. *J. CO2 Util.* **2017**, *21*, 119–131. [CrossRef]
41. Steiner, S.; Lothenbach, B.; Proske, T.; Borgschulte, A.; Winnefeld, F. Effect of relative humidity on the carbonation rate of portlandite, calcium silicate hydrates and ettringite. *Cem. Concr. Res.* **2020**, *135*, 106116. [CrossRef]
42. Zhan, B.J.; Xuan, D.X.; Poon, C.S.; Shi, C.J. Mechanism for rapid hardening of cement pastes under coupled CO_2-water curing regime. *Cem. Concr. Compos.* **2019**, *97*, 78–88. [CrossRef]
43. Gervais, C.; Garrabrants, A.C.; Sanchez, F.; Barna, R.; Moszkowicz, P.; Kosson, D.S. The effects of carbonation and drying during intermittent leaching on the release of inorganic constituents from a cement-based matrix. *Cem. Concr. Res.* **2004**, *34*, 119–131. [CrossRef]
44. Papadakis, V.G.; Vayenas, C.G.; Fardis, M.N. A reaction engineering approach to the problem of concrete carbonation. *AIChE J.* **1989**, *35*, 1639–1650. [CrossRef]
45. Sandoval, G.F.B.; Pieralisi, R.; Dall Bello de Souza Risson, K.; Campos de Moura, A.; Toralles, B.M. Clogging phenomenon in pervious concrete (PC): A systematic literature review. *J. Clean. Prod.* **2022**, *365*, 132579. [CrossRef]
46. Coughlin, J.P.; Campbell, C.D.; Mays, D.C. Infiltration and clogging by sand and clay in a pervious concrete pavement system. *J. Hydrol. Eng.* **2012**, *17*, 68–73. [CrossRef]
47. Kia, A.; Wong, H.S.; Cheeseman, C.R. Clogging in permeable concrete: A review. *J. Environ. Manag.* **2017**, *193*, 221–233. [CrossRef] [PubMed]
48. Pratt, C.J.; Mantle, J.D.G.; Schofield, P.A. UK research into the performance of permeable pavement, reservoir structures in controlling stormwater discharge quantity and quality. *Water Sci. Technol.* **1995**, *32*, 63–69. [CrossRef]

49. Hu, H.-H.; Zuo, X.-B.; Cui, D.; Tang, Y.-J. Experimental study on leaching-abrasion behavior of concrete in flowing solution with low velocity. *Constr. Build. Mater.* **2019**, *224*, 762–772. [CrossRef]
50. Beddoe, R.E.; Müllauer, W.; Heinz, D. On leaching mechanisms of major and trace elements from concrete—Carbonation, exposure to deicing salt and external sulphates. *J. Build. Eng.* **2022**, *45*, 103435. [CrossRef]
51. Edition, F. Guidelines for drinking-water quality. *WHO Chron.* **2011**, *38*, 104–108.
52. Horabik, J.; Molenda, M. *Encyclopedia of Agrophysics*; Gliński, J., Horabik, J., Lipiec, J., Eds.; Springer: Dordrecht, The Netherlands, 2011.
53. Gollmann, M.A.C.; da Silva, M.M.; Masuero, Â.B.; dos Santos, J.H.Z. Stabilization and solidification of Pb in cement matrices. *J. Hazard. Mater.* **2010**, *179*, 507–514. [CrossRef]
54. Lee, D. Formation of leadhillite and calcium lead silicate hydrate (C–Pb–S–H) in the solidification/stabilization of lead contaminants. *Chemosphere* **2007**, *66*, 1727–1733. [CrossRef]
55. Holmes, R.R.; Hart, M.L.; Kevern, J.T. Removal and breakthrough of lead, cadmium, and zinc in permeable reactive concrete. *Environ. Eng. Sci.* **2018**, *35*, 408–419. [CrossRef]
56. Lange, L.C.; Hills, C.D.; Poole, A.B. Preliminary Investigation into the Effects of Carbonation on Cement-Solidified Hazardous Wastes. *Environ. Sci. Technol.* **1996**, *30*, 25–30. [CrossRef]
57. Alexander, M.; Bertron, A.; De Belie, N. *Performance of Cement-Based Materials in Aggressive Aqueous Environments*; Springer: Dordrecht, The Netherlands, 2013.
58. Beddoe, R.E.; Dorner, H.W. Modelling acid attack on concrete: Part I. The essential mechanisms. *Cem. Concr. Res.* **2005**, *35*, 2333–2339. [CrossRef]
59. Wu, H.; Liu, Z.; Sun, B.; Yin, J. Experimental investigation on freeze–thaw durability of Portland cement pervious concrete (PCPC). *Constr. Build. Mater.* **2016**, *117*, 63–71. [CrossRef]
60. Xiang, J.; Liu, H.; Lu, H.; Gui, F. Degradation mechanism and numerical simulation of pervious concrete under salt freezing-thawing cycle. *Materials* **2022**, *15*, 3054. [CrossRef] [PubMed]

Disclaimer/Publisher's Note: The statements, opinions and data contained in all publications are solely those of the individual author(s) and contributor(s) and not of MDPI and/or the editor(s). MDPI and/or the editor(s) disclaim responsibility for any injury to people or property resulting from any ideas, methods, instructions or products referred to in the content.